

Major Activity of NewSUBARU

1. Imaging for Stress Corrosion Cracking in Stainless Steel with Laser Compton Scattering γ -ray

Stress corrosion cracking (SCC), a defect occurring in structures of nuclear power plants or chemical plants, has very intricate ramification and produces narrow cracks. Thus far, it has been difficult to observe the actual 3D SCC shape of small specimens. Therefore, we performed an imaging experiment using γ -ray for large specimens (a few dozens of mm thick). SUS316L stainless steel samples were used as specimens in this imaging experiment. In each specimen, SCC was artificially developed in high-pressure pure hot water at 300°C. The imaging experiment was performed using γ -ray in NewSUBARU BL-1A. Figure 1 shows the experimental equipment used. In this experiment, γ -ray was generated by the collision between a CO₂ laser and electrons. Imaging measurement using 1.76 MeV γ -ray was performed for stainless steel specimens with SCC or artificial slit. A clear slit image was confirmed for a stainless steel specimen up to 30 mm thick. On the other hand, an SCC image was confirmed for a 10-mm-thick specimen, although the image was not as clear as that shown in Fig. 2. The result indicates that laser Compton scattering γ -ray imaging may be a good non-destructive defect detection technique compared with ultrasonic testing.

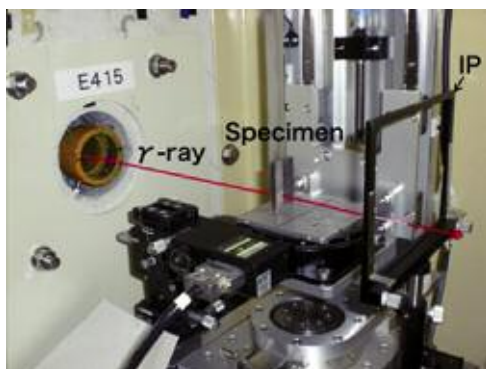


Fig. 1. Experimental equipment.

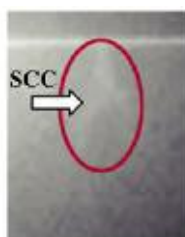
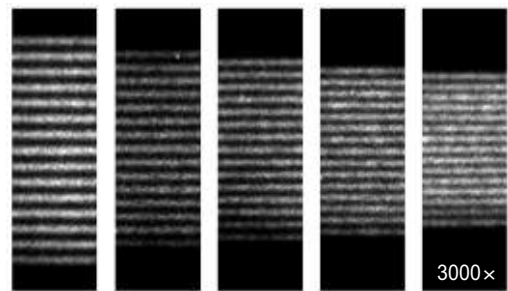


Fig. 2. Image of SCC in SUS316L specimen.

2. Imaging Performance Improvement of an Extreme Ultraviolet Microscope

The extreme ultraviolet microscope (EUVM) has been developed for the actinic mask inspection of an EUV finished mask and an EUV blank mask. Using this microscope, amplitude defects on a finished mask and phase defects on a glass substrate are observed. However, it has a problem of low contrast, which originates from (i) the thermal noise of a charge-coupled device (CCD) camera, (ii) wave aberrations of an optical component, and (iii) a non-uniform illumination intensity. To resolve these issues, EUVM was improved. (i) To reduce thermal noise, a cooled CCD camera was installed. (ii) To remove wave aberrations of a back-end turning mirror, a Mo/Si multilayer-coated thick glass substrate with a high surface accuracy was employed instead of a Si wafer substrate. Furthermore, *in situ* alignment was carried out to remove wavefront aberrations for a Schwarzschild imaging optics. In addition, (iii) by installing a scanning system on the front-end turning mirror, a highly uniform illumination intensity was achieved. As a result, images of less than 100 nm without astigmatism were obtained and are shown in Fig. 3.



Half pitch	150	130	120	110	100 nm
Contrast	0.34	0.26	0.25	0.22	0.18

Fig. 3. EUVM images of 150-, 130-, 110- and 100-nm-hp patterns and their contrast values.

3. Fabrication of X-ray Grating Using X-ray Lithography for X-ray Talbot Interferometry

X-ray radiographic imaging is very important in various fields such as medical, biological, inspection, and materials science. However, it is not sufficient to obtain clear X-ray images of samples with low absorbance materials, such as biological soft tissues. Thus, we used X-ray phase imaging method of an X-ray Talbot interferometer (XTI). In this method, X-ray gratings are required to have a narrow pitch and a high aspect ratio structure. Therefore, we fabricated X-ray gratings with a pitch of $5.3\ \mu\text{m}$ and a large effective area of $60 \times 60\ \text{mm}^2$ for X-ray Talbot interferometry. A carbon wafer as a membrane material of an X-ray mask was used to solve problem of the heat transformation of the membrane that happened at the time of X-ray exposure, as shown in Fig. 4. To make a higher aspect ratio X-ray grating, we developed a fabrication process composed of X-ray lithography and micro-electroforming method. In X-ray lithography, sticking was observed because of surface tension. Therefore, to avoid the sticking, the top surface of X-ray grating was modified by overexposure. The result showed that a resist structure with a high aspect ratio and a narrow pitch was obtained without surface tension in a large area. After Au electroforming, a large area and narrow pitch X-ray grating was fabricated, as shown in Fig. 5.

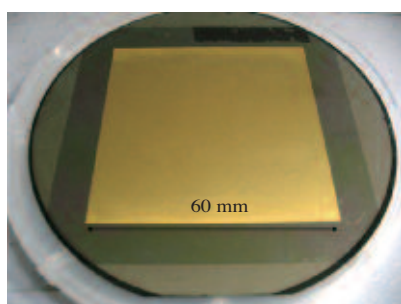


Fig. 4. Photograph of carbon X-ray mask.

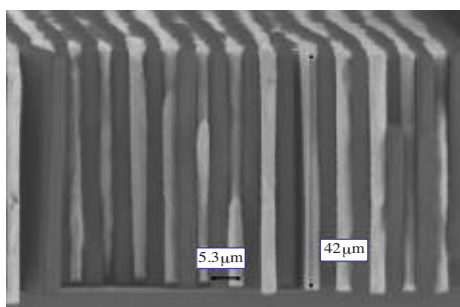


Fig. 5. SEM image of X-ray grating in cross section.

4. High-Precision Analysis for Material Analysis Beamline at BL-5 for Industrial Enterprises

A material analysis beamline for industrial enterprises was completed at BL-5 in March 2008. BL-5 consists of two branch lines, a double-crystal monochromator beamline (BL-5A) for use in the higher-energy region (1300-4000 eV) and a varied line spacing plane grating (VLSPG) monochromator beamline (BL-5B) for use in the lower-energy region (50-1300 eV), that cover the whole energy range of the soft X-ray region from 50 eV to 4000 eV. Both branch lines can be operated simultaneously. X-ray absorption fine structure (XAFS) measurements of total electron yield (TEY) and fluorescence yield (FLY) can be performed at BL-5A and BL-5B. In addition, X-ray photoelectron spectra (XPS) can be measured at BL-5B. We measured standard samples by the TEY method at BL-5B and obtained absorption spectra in each grating, i.e., 100 or 300 or 800 lines/mm. Figure 6 shows the boron *K*-edge near-edge X-ray absorption fine structure (NEXAFS) spectra of *h*-BN. The spectrum has been normalized to I_0 and had the linear pre-edge background removed. For *h*-BN, an intense peak at 191 eV appeared clearly in Fig. 6, which is assigned to transition from B1s to the unoccupied B2p π^* , the spectrum of which was of the same shape as that reported by Jiménez *et al.* [1].

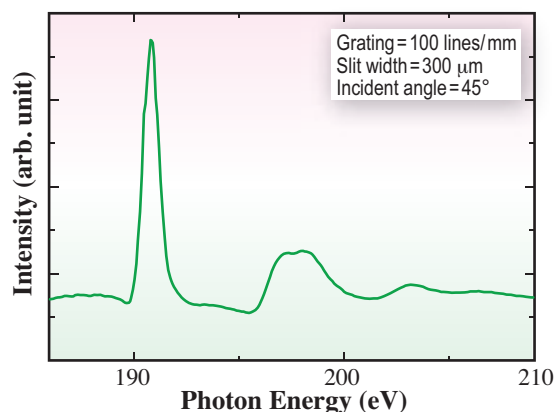


Fig. 6. *h*-BN B *K*-edge NEXAFS spectrum.

References

- [1] I. Jiménez *et al.*: Phys. Rev. **B55** (1997) 12027.